Activation of hydrogen and methane by thermalized FeO$^+$ in the gas phase as studied by multiple mass spectrometric techniques[1]

Detlef Schröder[a],*, Helmut Schwarz[a], David E. Clemmer[b], Yumin Chen[b],
P. B. Armentrout[b], Vladimir I. Baranov[c], Diethard K. Böhme[c]

[a]*Institut für Organische Chemie der Technischen Universität Berlin, Straße des 17. Juni 135, D-10623 Berlin, Germany*
[b]*Department of Chemistry, University of Utah, Salt Lake City, UT 84112, USA*
[c]*Department of Chemistry, York University, 4700 Keele Street, North York, Ont., M3J 1P3, Canada*

Abstract

The ion–molecule reactions of thermalized iron-oxide cation FeO$^+$ with dihydrogen and methane have been studied by three different experimental techniques: Fourier transform ion cyclotron resonance (ICR), guided ion beam (GIB), and selected-ion flow tube (SIFT) mass spectrometry. Although these studies agree in a qualitative sense, i.e., FeO$^+$ brings about activation of H$_2$ and CH$_4$ with quite low efficiencies, there exists a considerable quantitative divergence as far as rate constants and branching ratios are concerned. The sources of error in these three related, but yet different experimental techniques are analyzed and critically reviewed. This error analysis brings the data to internal consistency with each other, once an accurate reference is used for calibration. In general, the rate constants obtained with the SIFT apparatus appear as the most accurate ones, while those obtained under ICR conditions are slightly too large, and the rate constants determined with the GIB instrument are somewhat lower than SIFT. However, the branching ratios for the formation of Fe$^+$ and FeOH$^+$ in the reaction of FeO$^+$ with methane are subject to more subtle effects. In the SIFT apparatus, termolecular stabilization of the intermediates causes differences from the ICR and GIB measurements, which were obtained under single-collision conditions. © 1997 Elsevier Science B.V.

Keywords: FTICR-, GIB-, and SIFT mass spectrometry; Ion–molecule reactions; Iron oxide cation

1. Introduction

The reactions of bare FeO$^+$ cations with hydrogen [1–4] and methane [1,4–7] in the gas phase have been studied repeatedly during the last few years by various mass spectrometric techniques. This considerable interest is due to the fact that these reactions represent simple gas phase models for the oxidation of hydrocarbons by transition-metal oxenoids in the condensed phase [8].

In fact, metal oxenoids are of outstanding importance for several industrial and biochemical processes [9,10], and the role of concepts that may guide the development of new oxidation catalysts can hardly be overemphasized [11]. In this respect, the reaction mechanisms of transformations as simple as the ones described in Eq. (1) and Eq. (2) are fundamental for the understanding of transition-metal mediated oxidation of hydrocarbons in general.

$$FeO^+ + H_2 \rightarrow Fe^+ + H_2O \qquad (1)$$

$$FeO^+ + CH_4 \rightarrow Fe^+ + CH_3OH \qquad (2)$$

---
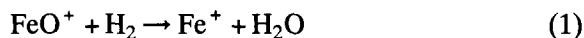
* Corresponding author.
[1] Dedicated to Fulvio Cacace on the occasion of his 65th birthday.

Both reactions are exothermic with reaction enthalpies of $\Delta H_R^0 = -37$ kcal mol^{-1} and -9 kcal mol^{-1}, respectively [12]. According to high-level ab initio studies [13], the reactant FeO$^+$ exhibits a sextet ground state ($^6\Sigma^+$). Because the ground state of bare Fe$^+$ is also a sextet (^{6}D) while H$_2$, H$_2$O, CH$_4$, and CH$_3$OH are singlets, reactions 1 and 2 may proceed entirely on sextet surfaces. However, experimental [3] and theoretical [13]b findings suggest that both reactions involve intermediate curve crossings to the corresponding quartet surfaces as illustrated in Fig. 1 [14] because the respective transition structures as well as the insertion intermediates R-Fe$^+$-OH (R = H, CH$_3$) are energetically favored on the low-spin surface.

Reactions 1 and 2 have already been studied independently in our three laboratories by three entirely different experimental techniques [2–4]: (i) ion cyclotron resonance (ICR) [15] (ii) guided ion beam (GIB) [16], and (iii) selected-ion flow tube (SIFT) mass spectrometry [17]. All three methods reveal that both exothermic processes occur at thermal energies [18]. What is exceptional about these reactions is that the magnitudes of the rate constants are only about 1% of the gas kinetic collision rate for reaction 1 and about 10% for reaction 2, as confirmed by all three

techniques. In view of the reaction exothermicities, reactions 1 and 2 are surprisingly inefficient (particularly reaction 1), and this points toward the operation of significant kinetic barriers. Despite this qualitative agreement, the quantitative comparison of the results is not satisfactory and indicates the operation of systematic errors in one or more of the different experimental approaches. Because of the wide application of these three experimental methods for the study of gas phase ion–molecule reactions, a detailed discussion of the potential sources of error is indicated, in particular with regard to the determination of rate constants, product distributions, and ion temperatures. Therefore, we have combined our efforts in this comparative study by examining the two elementary reactions 1 and 2, which are not only fundamental for catalysis, but also represent models for the interplay between "classical" transition structures on a single spin-surface and transition-metal mediated curve crossings between surfaces of different spin multiplicities [14].

2. Experimental section

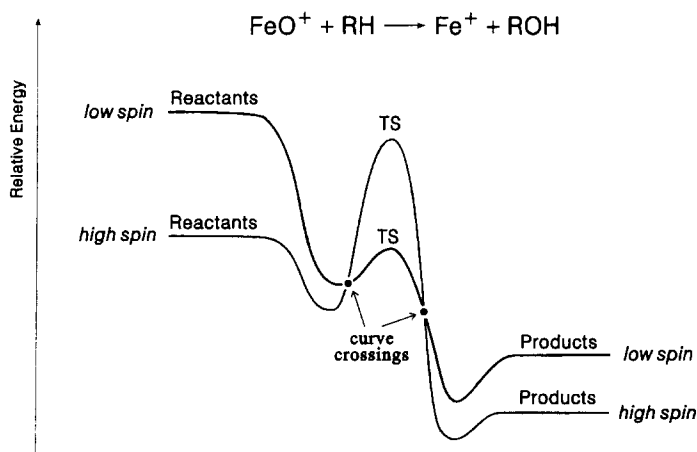The experiments were performed with Fourier transform (FT) ICR-, GIB-, and SIFT mass

Fig. 1. Qualitative potential-energy surface for low- and high-spin multiplicities in the reaction of iron-oxide cation with a substrate R-H (R = H, alkyl). TS: transition structure. For further details, see [13]b,[14].

spectrometers. Because the instruments and their operation have been described in detail before [15–17], here, we limit ourselves to the essential features. In a comparative study such as presented here for the ion–molecule reactions 1 and 2, it is of crucial importance to point out differences in these experimental approaches (Table 1). Furthermore, we pay particular attention to the methods used for ion production, ion thermalization, mass selection, and ion detection, respectively.

2.1. ICR

In these experiments, bare Fe^+ cations were generated by laser desorption/laser ionization of an iron target in the external ion source of a Spectrospin CMS47X Fourier-Transform ICR mass spectrometer [15]. Then, the cations were transferred to the analyzer cell and trapped in the field of a superconducting magnet (7 Tesla), using voltages of ca. + 1 V on the trapping plates perpendicular to the field. Mass selection of the ions of interest was achieved using the FERETS technique [19], a computer-controlled routine which combines frequency sweeps and single frequency shots to optimize ion isolation. For the generation of FeO^+, first the $^{56}Fe^+$ isotope was mass selected, then reacted with pulsed-in N_2O [20], and finally, $^{56}Fe^{16}O^+$ was mass selected; the high mass resolution of the FTICR excludes isobaric interferences within 0.001 amu. Due to the ionization processes as well as

the injection of the ions from the external source into the analyzer cell, the ions exhibit a considerable amount of kinetic and internal energy. In order to afford ion thermalization, argon was pulsed-in several times (up to 10 000 collisions) and FeO^+ was carefully re-isolated afterwards to avoid unintentional ion excitation. Ion–molecule reactions were followed by monitoring the time dependencies of the ion intensities after mass selection in the presence of a static pressure of the reactant gases (i.e. hydrogen or methane), and the data were analyzed in terms of pseudo-first-order kinetics. Ion thermalization was assumed to be complete, when neither endothermic processes nor deviations from strictly linear kinetics were observed and further increase of the number of thermalizing collisions did not affect the experimentally measured rate constants. For reactions 1 and 2, the kinetics were linear for more than two orders of magnitude, and the experimental error of these relative rate constants is ± 5%. The rate constants given here for reactions 1 and 2 are averages of at least four independent measurements. The relative rate constants were converted to absolute rate constants by calibrating the pressure measurement of the ion gauge (IMG 070, Balzers, Liechtenstein) on the basis of well-known ion–molecule reactions. Further, the relative sensitivities [21] of the ion gauge for the reactant gases were taken into account. Due to the strength of the magnetic field in the 7 Tesla version of the CMS47X, the most frequently used calibration reactions (e.g.

Table 1
Different instrumental features in the examination of ion–molecule reactions in ion–cyclotron resonance (ICR), guided–ion beam (GIB), and selected ion–flow tube (SIFT) mass spectrometers

	Thermalizing collisions	Pressure regime[a] (mbar)	Collision frequency (s^{-1})	Interaction time (s^{-1})	Calibration
ICR	$0–10^{4}$ [b]	$< 10^{-6}$	< 1	$10^{-2}–10^{2}$	Relative
GIB	$\sim 10^{5}$ [c]	$\sim 10^{-3}$	$\sim 10^{3}$	10^{-4}	Absolute
SIFT	$\sim 10^{5}$	~ 0.5	$\sim 10^{7}$	10^{-2}	Absolute

[a] Pressure in the interaction region where the ion–molecule reaction of interest takes place.

[b] Depending on the pulsed-valve sequence.

[c] Note that source and reaction zones are physically separated in GIB, such that the pressure regime for reactions differs from the region where thermalizing collisions occur.

$CH_4^{+\cdot}$ + CH_4 or $O_2^{+\cdot}$ + CH_4 [22]) could *not* be employed, because any ions below m/z = 17 amu can neither be handled nor detected. Therefore, other ion–molecule reactions were studied [23], and the reactions Ar^+ + H_2 and Fe^+ + N_2O were used as benchmarks for calibration (see below). The errors associated with the literature values for these rate constants, the accuracy of the pressure measurements and the calibration procedure increase the error of ± 5% for the experimentally measured relative rate constants up to ± 30% in terms of absolute rate constants [24]. The accuracy is particularly low for reactions of hydrogen, because the relative sensitivity of the ion gauge for this gas is low [21], such that the error increases to ± 40% in this case.

2.2. GIB

In the GIB experiments, FeO^+ was produced in a flow tube source described in detail previously [16]b,[25]. First, Fe^+ is generated in a d.c. discharge by 1.5–3.0 keV Ar ion impact on a rod of carbon steel. The ions were then swept down a meter long flow tube by He and Ar flow gases maintained at pressures of ~0.60 and ~0.06 mbar, respectively. Generation of FeO^+ was achieved by admitting N_2O or NO_2 to the flow tube. N_2O was injected into the source region of the instrument at pressures less than 1 mbar such that FeO^+ was formed in the energetic plasma near the discharge region of the source. The overall reaction of Fe^+ with N_2O is exothermic by 1.80 ± 0.06 eV [26] as has been discussed previously [27]. To further limit the internal energy of the FeO^+ produced, this ion was also formed by the interaction of Fe^+ with NO_2, introduced ~50 cm downstream of the source, a process that is exothermic by only 0.35 ± 0.06 eV [26]. In both methods, we calculate that the ions undergo ~10^5 collisions with He and ~10^4 collisions with Ar before exiting the flow tube. The many collisions with the carrier gases should thermalize the FeO^+ ions

produced with respect to electronic, vibrational, and rotational states. Indeed, results of these experiments for FeO^+ produced by reaction with both N_2O and NO_2 were identical within experimental uncertainty. In addition, collision-induced dissociation (CID) of FeO^+ with Xe indicated that the ions were not internally excited [28]. Further, no changes in reactivity of the FeO^+ beam were observed when H_2 or O_2 were added to the flow tube to effect additional cooling. We assume that these ions have equilibrated to the ca. 300 K temperature of the flow gasses. Previous work from this laboratory [25,29] has shown that this assumption is reasonable.

The accuracies of the cross sections obtained with the GIB instrument are determined by several factors. Cross sections are obtained by converting product and reactant ion intensities using the formula, $I_r = (I_r + \sum I_p)e^{(-n\sigma l)}$ and $\sigma_p = \sigma I_p / \sum I_p$, where I_r is the measured intensity of the reactant ions, I_p is the measured intensity of the product ions, the summation is over the various product ions, n is the number density of the neutral reactant, and l is the length of the interaction region. In early work, we determined that the effective gas cell length calculated for the geometry of our gas cell gave absolute cross sections in good agreement with both other experiments and theory, and we assign a conservative error of ± 10% to this value. Pressure measurements of the neutral gas are made with a capacitance manometer and corrected for thermal transpiration effects such that a conservative error is ± 10%. The temperature of the neutral gas is ambient and therefore has a small uncertainty. Thus, the overall error in the measurements is assigned as ± 20%. Systematic errors that vary from system to system can occur in the measurement of the ion intensities. A Daly-type secondary electron, scintillation detector with a 28 kV primary dynode is used to measure ion intensities. For the light ions measured here, such a device should give nearly 100% detection efficiency. Some detection difficulties can occur if ions are not efficiently transported to the

detector, but the use of an octopole ion beam guide reduces such problems very effectively. Mass discrimination in the quadrupole mass filter could also limit the efficient transport of ions to the detector, but operation of the quadrupole at low mass resolution minimizes such difficulties. Neither of these latter two procedures guarantee that ion collection problems are eliminated.

The conversion of cross sections to rate constants is straightforward and absolute. This is achieved using the formula, $k(\langle E \rangle) = v \cdot \sigma(E)$, where $\langle E \rangle = E + 3\gamma kT/2$ is the effective energy of the ion/neutral interaction, $v = (2E/\mu)^{1/2}$ is the relative velocity of the reactants at energy E, μ is the reduced mass of the reactants, and $\gamma = m/(m + M)$ with m and M as the masses of the reactant ion and neutral, respectively. As E approaches zero, $k(\langle E \rangle)$ approaches the thermal rate constant at an effective temperature of $T' = \gamma T$. We ordinarily attribute the same absolute error used in the cross sections to the rate constants, $\pm$ 20%, although this assumes that the uncertainty of the relative velocity is small.

2.3. SIFT

In the SIFT experiments [17], FeO$^+$ was derived from a 1:100 mixture of Fe(CO)$_5$ and N$_2$O in a high-pressure chemical-ionization source at an electron energy of 50 eV. FeO$^+$ was mass selected with a quadrupole mass filter, injected into flowing helium gas at 0.46 $\pm$ 0.01 mbar with an injection energy of less than 2 eV and then allowed to thermalize by ca. (2–4) $\times$ 10^5 collisions with He atoms before entering the reaction region.

The SIFT technique provides absolute rate constants and their determination requires accurate knowledge of reactant concentrations, reaction times, and diffusional losses. The major errors arise from uncertainties in the neutral flow-rate (< $\pm$ 10%), the average buffer–gas flow velocity ($\pm$ 5%), the effective reaction length ($\pm$ 2%) and the slope of the semi-logarithmic reactant ion decay (usually < $\pm$ 5%). The total error assigned to the determination of

absolute rate constants is thus $\pm$ 22%, although we normally quote $\pm$ 30%. The relative accuracy of the rate constants of two different reactions is estimated as $\pm$ 15%.

The determination of branching ratios for reactions with more than one product ion depends on a knowledge of any mass discrimination in the detection system. The extent of mass discrimination can be evaluated from the observed mass balance between reactant and product ions. For the reaction of FeO$^+$ with H$_2$, HD, and D$_2$ exact balance was observed between the initial FeO$^+$ signal and the final signal of the Fe$^+$ product. This was to be expected since discrimination in the mass analysis with the downstream quadrupole, as well as in the detection of the ions with the channeltron electron multiplier, is expected to be negligible for these two ions of not too dissimilar mass. Similar considerations apply to the reaction of FeO$^+$ with CH$_4$ in which Fe$^+$ and FeOH$^+$ (or FeOH(CH$_4$)$^+$ by secondary reaction) are the observed product ions. The accuracy of the branching ratio for this reaction is conservatively estimated to be < $\pm$ 5%.

3. Reaction of FeO$^+$ with H$_2$, HD, and D$_2$

In this section, we present the experimental findings obtained in ICR, GIB, and SIFT mass spectrometry for the reactions of FeO$^+$ with H$_2$, HD, and D$_2$, respectively, and discuss them in detail in order to arrive at internal consistency with respect to effective ion temperatures and absolute rate constants for reaction 1.

3.1. Results

The reaction of FeO$^+$ and H$_2$ has three features which are observed in all instruments. These are summarized before comparing the differences in the experimental findings: (i) The rate constant (k_{H_2}) of reaction 1 is rather low as compared to

Table 2

Rate constants k (in 10^{-12} cm^3 s^{-1}) and kinetic isotope effects (KIE) for the reactions of FeO$^+$ with H$_2$, HD, and D$_2$, respectively, in the ICR, GIB, and SIFT experiments

	k_{H_2}	k_{HD}	k_{D_2}	KIE(H$_2$/HD)[a]	KIE(H$_2$/D$_2$)[a]
ICR[b]	16 ± 6[c]	13 ± 5	11 ± 6	0.98 ± 0.4	1.08 ± 0.4
ICR[d]	10 ± 4	8.1 ± 3.2	6.9 ± 2.8	0.98 ± 0.4	1.08 ± 0.4
GIB[e]			2.5 ± 1.0		
SIFT[f]	8.8 ± 2.6	7.7 ± 2.3	4.2 ± 1.3	0.94 ± 0.25	1.54 ± 0.4

[a] The KIEs are corrected for different collision frequencies of H$_2$, HD and D$_2$, respectively.
[b] [2].
[c] An independent re-measurement gave k_{H_2} = (14 ± 5) × 10^{-12} cm^3 s^{-1}.
[d] Re-calibrated values, see text.
[e] Corrected value according to [3]; also see [4].
[f] [4].

the collision rate constant (k_C = 1.5 × 10^{-9} cm^3 s^{-1}); (ii) Although hydrogen is activated by FeO$^+$, the intermolecular kinetic isotope effects with respect to the reaction efficiencies (k/k_C) for H$_2$, HD and D$_2$ are small and close to unity [2,4]; (iii) The formation of FeOH$^+$ + H$^.$ exhibits a kinetic threshold [2,3] and does not occur at thermal energies [4]. However, the experimentally measured rate constants for reaction 1 and its isotopologues differ significantly (Table 2), and we will next discuss these deviations in more detail.

The previous ICR experiments [2] on the reactivity of FeO$^+$ with H$_2$, HD, and D$_2$ resulted in rate constants of k_{H_2} = (1.6 ± 0.6) × 10^{-11} cm^3 s^{-1}, k_{HD} = (1.3 ± 0.5) × 10^{-11} cm^3 s^{-1}, and k_{D_2} = (1.1 ± 0.4) × 10^{-11} cm^3 s^{-1}, respectively. After publication of the lower rate constants obtained in the GIB and the SIFT experiments [3,4], the ICR experiments were repeated and reaction 1 was monitored over several orders of magnitude (Fig. 2). Notwithstanding, we still obtain a rate constant of k_{H_2} = (1.4 ± 0.5) × 10^{-11} cm^3 s^{-1} when the same calibration scheme is applied as we have used before (see below). Further, we considered the possibility of mass discrimination effects due to the ion detection in ICR and data processing in the Fourier transform procedure [30]. Provided that the excitation windows for ion detection and the excitation amplitudes are chosen properly and a sufficient data

size for recording the transient as well as for subsequent transformations is provided, mass discrimination effects are minor and within the range of the statistical error of the experiments (± 5%).

Only the reaction of FeO$^+$ with D$_2$ was studied in the GIB experiments in order to enhance mass resolution while not limiting ion collection efficiency. Fig. 3 shows the dependence of k_{D_2} from the kinetic energy of FeO$^+$ as obtained
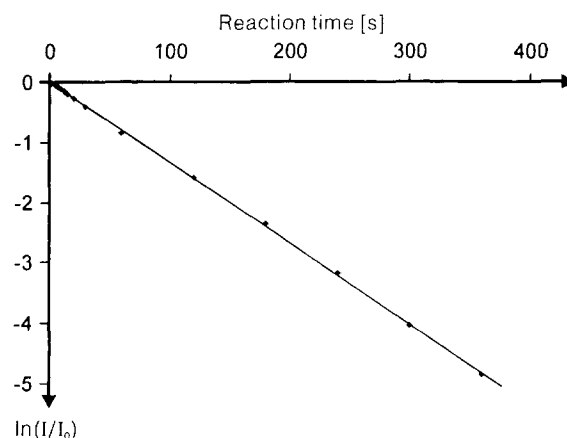

Fig. 2. Pseudo first-order kinetic data for reaction 1 in the ICR mass spectrometer. Logarithm of the fraction of the intensity (I) of FeO$^+$ relative to I_0 at a reaction time t = 0; p(H$_2$) = 1.4·10^{-8} mbar. The last entry in the graph corresponds to more than 99% conversion of the FeO$^+$ reactant ion. The slope corresponds to a relative rate constant of 0.0134 s^{-1} (± 5%) and the new calibration leads to an absolute rate constant of (9.6 ± 3.8) × 10^{-12} cm^3 s^{-1} for this particular experiment.

from the conversion of the cross sections to thermal rate constants. The most intriguing finding is that in the vicinity of the threshold the cross section diminishes with increasing energy; this observation can be interpreted in terms of a negative temperature dependence [31] of the rate constant of reaction 1. At an effective collision energy of 0.04 eV, which roughly corresponds to room temperature, a rate constant of k_{D_2} = (2.5 ± 1.0) × 10^{-12} cm^3 s^{-1} was found for the reaction of FeO$^+$ with deuterium. The uncertainty includes the scatter in the data at this energy, the 20% uncertainty in the cross sections, and a 30% uncertainty in the velocity at this energy. A lower rate constant (k_{D_2} = 1.5 × 10^{-12} cm^3 s^{-1}) was previously reported [3]; however, this value included the anomalously low values shown in Fig. 3 (open circles). However, the experimental errors in GIB measurements may increase the lower the energies are, because the transmission through the octopole diminishes upon approaching zero field. Further, the previous GIB data [3] demonstrate that formation of FeOD$^+$ + D$^{\cdot}$ has a kinetic threshold of ca.

0.5 eV, thereby explaining the absence of this product ion in the ICR and SIFT experiments.

The SIFT experiments are in good agreement with the ICR data as far as reaction products and the trends in the rate constants for the reactions of FeO$^+$ with H$_2$, HD, and D$_2$ are concerned, i.e., k_{H_2} = (8.8 ± 2.6) × 10^{-12} cm^3 s^{-1}, k_{HD} = (7.7 ± 2.3) × 10^{-12} cm^3 s^{-1}, and k_{D_2} = (4.2 ± 1.3) × 10^{-12} cm^3 s^{-1}, respectively [32]. However, the absolute rate constants obtained with the SIFT technique are lower than the ICR results by approximately a factor of two. Interesting with respect to the potential-energy surface [13]b of reaction 1 is that even under the relatively high pressure (0.47 mbar) of helium, which can serve as a stabilizer in three-body association reactions, the formation of the adduct FeO$^+\cdot$H$_2$ is not observed under SIFT conditions. Collisional dissociation in the sampling region of any FeO$^+\cdot$H$_2$ which may have formed by three-body association cannot be completely ruled out in the SIFT experiments, although this seems unlikely.

3.2. Discussion

Certainly, the results of the three methods are in general agreement in that thermalized FeO$^+$ activates hydrogen to yield Fe$^+$ and water as products. Nevertheless, the quantitative agreement is still rather poor. What could be the origin(s) of these deviations?

First, it is worth stressing that none of the experiments involve highly excited FeO$^+$ ions: (i) According to the GIB experiments, the absence of formation of FeOH$^+$ clearly demonstrates that kinetically "hot" ions (greater than about 0.5 eV) are not present in the ICR and SIFT experiments; (ii) the energy dependencies of the cross sections for reaction 1 as studied by ICR and GIB are typical for exothermic ion–molecule reactions [2,3], namely, they have a negative temperature dependence [31] indicating that in part the lifetime of the encounter complex determines the rate constant. This effect would not have been observed if the FeO$^+$ were excited.
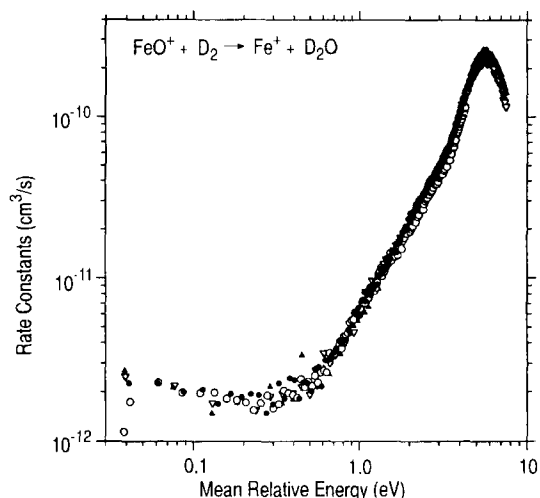

Fig. 3. GIB results for the variation of the rate constant k_{D_2} for the reaction of FeO$^+$ with D$_2$ to form Fe$^+$ and D$_2$O as a function of kinetic energy in the center-of-mass frame. Different symbols represent results from independent data sets. For the sake of clarity, other products formed at higher collision energies are omitted (see [3]).

Nevertheless, the lifetime of the encounter complex seems to be too small to allow for an effective cooling under SIFT conditions, because the $FeO^+·H_2$ adduct is not observed. This is a reasonable result given a theoretically predicted binding energy for FeO^+-H_2 of only 5 kcal mol^{-1} [13]b; (iii) The pseudo first-order kinetics are strictly linear in both ICR and SIFT experiments over several orders of magnitude. Participation of electronically excited states of FeO^+ is likely to result in a deviation from this behavior [33]; (iv) the different methods used for the generation of FeO^+ should not be responsible for the different rate constants, if the ions are properly thermalized before monitoring its reaction and the latter appears to be the case [3,4,34].

Therefore, the deviations of the measured rate constants of reaction 1 must be due to *systematic errors* in one or more of the three methods employed. The most obvious possible source of error is that associated with different effective ion temperatures and collision energies, respectively, in the three experiments. In almost all experimental set-ups which are used to study ion–molecule reactions, ion thermalization is a prerequisite, because the ionization techniques, e.g., electron ionization, are far above threshold when reasonably high ion currents are achieved. In addition, in ICR and GIB the ions are subjected to electromagnetic fields, while the ions float free in a SIFT set-up. Indeed, the simplicity of reaction 1 makes it a well-suited model system for the comparison of experimental techniques: FeO^+ is readily accessible, reaction 1 can easily be followed and has a single reaction product, and finally, the endothermic formation of $FeOH^+$ exhibits a clear-cut threshold and would always prevail when "hot" ions were present. Note however, that the GIB experiments demonstrate that the energy dependence of the rate constant—though significant—is not very dramatic in the low-energy regime (i.e. below 0.5 eV).

For various reasons, ion thermalization in ICR mass spectrometry has been a continuing subject

of controversy. The justified criticism is mainly due to the fact that in the low-pressure regime of ICR the effective number of thermalizing collisions cannot be as large as in GIB with a flow tube source and SIFT or similar techniques operating at much higher pressures. In this respect, the use of pulsed-valves for ion thermalization in ICR mass spectrometry is essential, as it allows monitoring of the efficiency of the thermalization process by studying rate constants at different numbers of thermalizing collisions concomitant with ion detection at rather low pressures after the pulsed-in buffer gases are pumped away. With respect to reaction 1, the most convenient procedure is to trap mass selected FeO^+ for a certain reaction time in a given pressure of hydrogen while monitoring the dependence of the conversion of FeO^+ to Fe^+ as a function of thermalizing collisions (viz. the number of gas pulses prior to re-isolation of the reactant ion). After ca. 5000 thermalizing collisions with argon [35], the rate constant of reaction 1 reaches a plateau and hence, we assume that thermalization is complete. This conclusion is further substantiated by the fact that intentional kinetic excitation of the FeO^+ ion leads to a decrease of the rate at low conversions [2], completely in line with the negative temerature dependence observed in the GIB experiments [3].

If, however, the ions are thermalized in the ICR measurement and mass discrimination is not severe, the deviation of the ICR rate constant from the GIB and SIFT data must have another origin. Therefore, we carefully analyzed other possible sources of error, in particular those associated with the conversion of the measured rate constants to absolute values. In this procedure, the determination of the real pressure of the neutral reactant is of crucial importance. Basically, the calibration reduces to two aspects of pressure measurement, namely, the relative sensitivity of the ion gauge to the gas of interest (i.e. molecular hydrogen) and the absolute calibration error of the ionization gauge. With

respect to the relative sensitivities, we completely relied on the data published by Bartmess and Georgiadis [21] and we used them for calibrating the Berlin ICR relative to established rate constants of a set of well-known ion–molecule reactions. However, in this procedure [24] two reactions were used as reference points which now turn out to be misleading.

$$Ar^+ + H_2 \rightarrow ArH^+ + H^. \qquad (3)$$

$$Fe^+ + N_2O \rightarrow FeO^+ + N_2 \qquad (4)$$
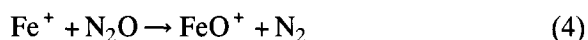
In the old calibration of the Berlin ICR [24] we used an averaged [36] rate constant of $k_3 = (1.1 \pm 0.3) \times 10^{-9}$ cm^3 s^{-1} for reaction 3, and our analysis of the whole set of data of ICR rate constants gave a measured $k_3 = (1.3 \pm 0.3) \times 10^{-9}$ cm^3 s^{-1} which was considered to be within the experimental error. However, the recent evaluation of gas-phase kinetics by Anicich [37] discards this value and rather recommends $k_3 = (8.9 \pm 1.8) \times 10^{-10}$ cm^3 s^{-1} which is almost out of error limits of our determination. Further, according to GIB this rate constant is $(9.5 \pm 2.0) \times 10^{-10}$ cm^3 s^{-1}, and also the different rates for Ar^+ ($^2P_{3/2}$) and Ar^+ ($^2P_{1/2}$), respectively, were considered [16]a. As a reference for a fast re-calibration of the ICR mass spectrometer (e.g. after venting the vacuum system), we used reaction 4 adopting a rate constant of $k_4 = 7 \times 10^{-11}$ cm^3 s^{-1} as determined by Kappes and Staley [20], and obtained $k_4 = (6.5 \pm 1.6) \times 10^{-11}$ cm^3 s^{-1} for this process [38]. However, recent SIFT results [4] suggest a significantly lower rate constant of only $k_4 = (3.1 \pm 0.9) \times 10^{-11}$ cm^3 s^{-1}. These findings suggest that the crucial references in the calibration of the Berlin ICR were wrong with the consequence that the absolute rate constants were somewhat too high. Inclusion of a number of other calibration reactions, e.g., reactions occurring at the collisional limit, leads to the conclusion that the rate constants determined by the Berlin group until mid 1995 were on the average too high by a factor of 1.4 ± 0.3. Thus, for reaction 1 the ICR value

reduces to $k_{H_2} = (1.0 \pm 0.4) \times 10^{-11}$ cm^3 s^{-1} which is in reasonable agreement with the SIFT result.

Because this re-calibration does not include all conceivable uncertainties (e.g. the deviation by a factor of two for the reaction $Fe^+ + N_2O$), one further observation is worth reporting: the set of calibration reactions revealed that part of the discrepancies may be due to the uncritical acceptance of the relative sensitivities published by Bartmess and Georgiadis [21] without considering differences due to the particular ion gauge used [39] and its positioning in the vacuum system [40]. Another potential source of error which has been completely neglected so far is due to the effusion of the reactant gas from the reservoir (up to 2 bar) into the high vacuum inside the analyzer (ca. 10^{-9} mbar) which may result in a cooling of the neutral reactant due to a Joule–Thompson effect; thus, though ions may be "hot" the neutrals may be "cold". These objections are fundamental and dependent on the nature of the neutral gas, pointing to the operation of yet imponderable systematic errors which cannot be compensated for simply by calibration. As a consequence, the accuracy of rate constants obtained with ICR will in general be lower than those from SIFT measurements, in which absolute rates are determined.

In the GIB experiments, thermalization is much less problematic because the flow tube source allows the ions to undergo several thousands of collisions prior to the measurement of their threshold behavior. Although there exist a few examples in which collisional cooling is ineffective [3,41,42], this is by no means inherent to GIB and also applies to ICR and SIFT. Another possibility for ion excitation in GIB is due to unintentional collisions with background gas during mass selection in which the ions are accelerated to a few hundred eV kinetic energy. In both cases, a small fraction of excited ions in the incident beam would then appear as a nonzero background in the cross section diagrams; however, this is definitely not observed for reaction 1. In fact, significant excitation of FeO^+

above room temperature can rigorously be excluded in this case because: (i) the cross section exhibits a negative temperature dependence, typical for an exothermic, lifetime-determined ion–molecule reaction and (ii) any excited FeO^+ ions should also lead to $FeOH^+$, which is not observed at the lowest energies. Due to the large exothermicity of reaction 1 (− 37 kcal mol^{-1}), there is the possibility of a large kinetic energy release. As the collection efficiency of the Fe^+ product could be adversely affected by such a large kinetic energy release (especially at low collision energies where the ions spend more time in the octopole beam guide), this effect could lead to an underestimation of the rate constant in the GIB measurements. Nonetheless, ion collection in the GIB instrument should be efficient at low energies, because even a kinetic energy release of 0.5 eV is comparable to the spread of energies for the incident FeO^+ beam (0.4 eV) when the cross sections are measured, and the width of the precursor beam is explicitly considered in the data analysis. At this point, we cannot evaluate the validity of this argument (see below), because so far it was not possible to generate metastable $FeO^+ \cdot H_2$ adducts and monitor the kinetic energy release associated with its dissociation by means of other mass spectrometric techniques.

Let us summarize the discussion: in the ICR, GIB, and SIFT experiments the reactivity of thermalized FeO^+ cations is probed (Table 1). Overall, the rate constant of $k_{D_2} = (2.5 \pm 1.0) \times 10^{-12}$ $cm^3 \, s^{-1}$ measured in the GIB experiment is somewhat lower, but within experimental error of the SIFT data ($k_{D_2} = (4.2 \pm 1.3) \times 10^{-12} \, cm^3 \, s^{-1}$), while slightly out of the error margins of the corrected ICR value ($k_{D_2} = (6.9 \pm 2.8) \times 10^{-12}$). Thus, ICR and GIB experiments can be brought to reasonable agreement with the SIFT results.

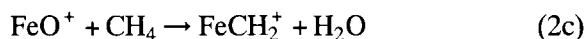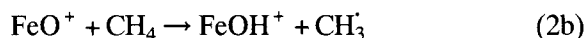### 3.3. Consequences for the mechanism of reaction 1

The convergence of the experimental data for

reaction 1 allows us to address the mechanism of the H-H bond activation by FeO^+ in further detail [14]. The present results settle the rate constant of reaction 1 and prove that it occurs at thermal energies. In view of the fact that reaction 1 is very exothermic, regardless whether Fe^+ (^6D)or Fe^+ (^4F) is formed, one is tempted to interpret the reaction efficiency of $k/k_C \approx 0.006$ in terms of an Arrhenius activation barrier associated with H-H bond activation, leading to a "classical" barrier of ca. 3 kcal mol^{-1} [4]. To the satisfaction of theoretical methods, this figure is in rather good agreement with the calculated activation energy of ca. 6 kcal mol^{-1} for the rate-determining transition structure which is located on the quartet surface of the $[Fe,H_2,O]^+$ system [13]b,[14]. However, if the assumption of an Arrhenius behavior is justified, the energy dependence of reaction 1 should reveal a threshold feature, even for this small barrier. This is not observed in the GIB experiments in that the cross section monotonically decreases with increasing collision energy below 0.2 eV (Fig. 3). Hence, the low reactivity of FeO^+ toward molecular hydrogen cannot be explained by a classical barrier along the potential energy surface, but is probably related to the inefficiency associated with switching between surfaces of different spin which occurs close to the thermochemical threshold [14]. This curve crossing may exhibit an entirely different energy or temperature dependence which is currently not clear, due to the lack of an appropriate theoretical description for the temperature dependence of two-state reactivity for transition-metal containing species.

4. Reactions of FeO^+ with CH_4

The second reaction we want to examine in more detail is that of FeO^+ with CH_4. Here, beside the rate constant, comparison of the different product channels that evolve must also be examined. The instrumental deviations of the rate constants of reaction 2 are similar to that for

reaction 1, hence, the discussion focuses on the effects of internal energy, mass resolution, and overall pressure on the measured branching ratios of the different products (Eq. (2a), (2b) and (2c)).

$$FeO^+ + CH_4 \rightarrow Fe^+ + CH_3OH \qquad (2a)$$

$$FeO^+ + CH_4 \rightarrow FeOH^+ + CH_3^{\cdot} \qquad (2b)$$

$$FeO^+ + CH_4 \rightarrow FeCH_2^+ + H_2O \qquad (2c)$$

4.1. Results

In the earlier ICR experiments [6,18], a rate constant of $k_{CH_4} = 2.0 \times 10^{-10}$ cm^3 s^{-1} was reported for the reaction of FeO$^+$ with CH$_4$. Further, three different reaction products were obtained in ICR, with FeOH$^+$ predominating over formation of Fe$^+$ (2a:2b = 41:57), and a minor pathway (2%) leading to the formation of FeCH$_2^+$ concomitant with water as neutral product (2c). For [D$_2$]- and [D$_4$]-methane as reactants, the labeled ions FeCHD$^+$ and FeCD$_2^+$ are formed, though in even smaller amounts (< 1%). At the time these experiments were made, the Berlin ICR was not fully calibrated and k_{CH_4} was simply determined relative to the rate for formation of FeO$^+$ from Fe$^+$ and N$_2$O (reaction 4) using the rate constant reported by Kappes and Staley [20], which later turned out [4] to be too high by a factor of two (see above).

Repetition of the ICR measurements and re-calibration of the rate constant as outlined above for the reaction 1 leads to a revised rate constant $k_{CH_4} = (8.5 \pm 2.6) \times 10^{-11}$ cm^3 s^{-1}. Careful examination of the branching ratio between reactions 2a and 2b fully confirms the previous results and leads to Fe$^+$:FeOH$^+$ = (39 ± 4):(61 ± 4) under ICR conditions. The formation of FeCH$_2^+$ was also observed in the low-percent regime (high resolution: m_{exp} = 69.9505895 amu, m_{calc} = 69.9505893 amu, $m/\Delta m$ = 3.5 × 10^8), but the signal was too low in intensity to allow for precise quantification of the reaction kinetics (see below). Even at long reaction

times, i.e. 6 min. at a CH$_4$ pressure of 1.8 × 10^{-8} mbar until complete conversion of FeO$^+$, neither Fe$^+$ nor FeOH$^+$ form the corresponding adduct ions with CH$_4$, which therefore obviously demand termolecular stabilization.

Fig. 4 shows the energy dependence of reaction 2 as obtained with the GIB instrument. Similar to reaction 1, in the beginning the efficiencies for the formation of FeOH$^+$ and Fe$^+$ decrease with increasing energy, thus, displaying a negative temperature dependence, which is again typical for an exothermic ion–molecule reaction with a significant kinetic bottleneck. Then at a threshold of ca. 0.6 eV, the reaction efficiency begins to rise again, and the Fe$^+$ channel becomes more and more favored. In the low-energy regime, the branching ratio between reactions 2a and 2b is strongly energy dependent in favor of FeOH$^+$ (Fig. 4). At the lowest energy (0.04 eV), the GIB measurements lead to k_{CH_4} = (2.8 ± 1.8) × 10^{-11} cm^3 s^{-1}. There is some experimental indication that this lowest energy data point is too low. Indeed, if the cross sections for both product channels are extrapolated from the data between 0.08 and 1.0 eV using a power
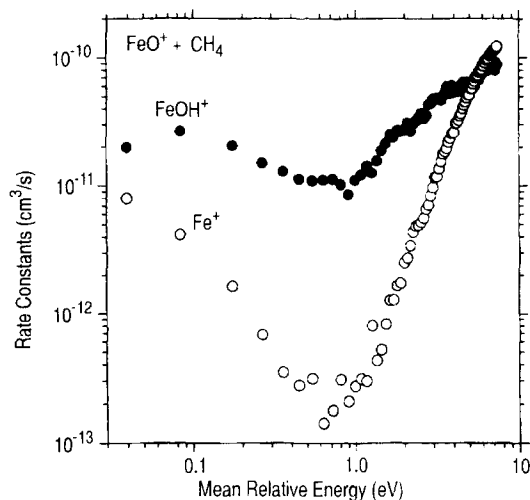

Fig. 4. GIB results for the variation of the rate constants k_{CH_4} for the reaction of FeO$^+$ with CH$_4$ to form FeOH$^+$ + CH$_3^{\cdot}$ (closed circles) and Fe$^+$ + CH$_3$OH (open circles) as a function of kinetic energy in the center-of-mass frame. For the sake of clarity, other products at higher collision energies (e.g. FeOCH$_3^+$) are omitted.

law (although this is not a rigorous expectation), the rate constants for $FeOH^+$ and Fe^+ are found to be 6.2 and 3.4×10^{-11} cm^3 s^{-1}, for a total rate constant of 9.6×10^{-11} cm^3 s^{-1}. This is most conservatively viewed as an upper limit to the true rate constant, but it agrees nicely with the ICR measurement. At thermal energies, the branching ratio of $Fe^+:FeOH^+$ = 29:71 is obtained, but the extrapolated values yield 36:64, again in somewhat better agreement with the ICR results. In contrast to the ICR results,

even upon careful inspection the formation of cationic iron carbene, $FeCH_2^+$, is not observed within the experimental accuracy either at low or at higher collision energies. A conservative upper limit to the cross section for $FeCH_2^+$ is 0.2×10^{-16} cm^2, or < 0.2% of the products at thermal energies.

Under SIFT conditions, the decay of FeO^+ is perfectly linear over almost three orders of magnitude (Fig. 5), and $FeOH^+$ and Fe^+ are formed as ionic products; again, formation of $FeCH_2^+$
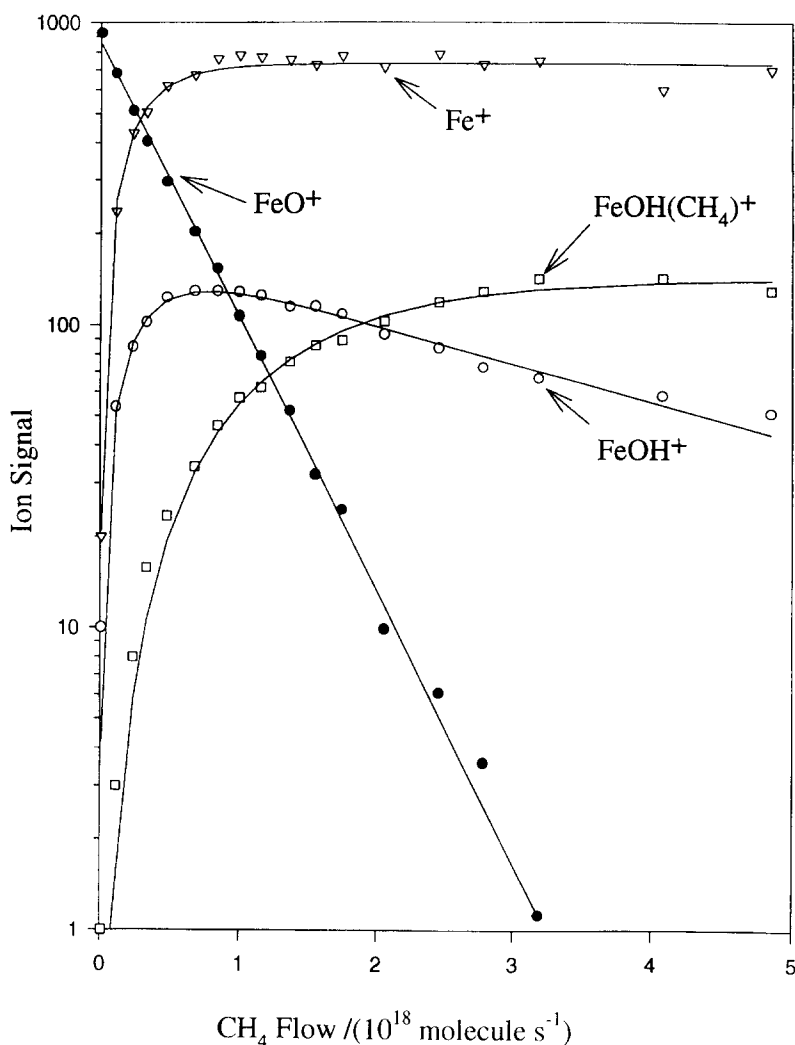

Fig. 5. SIFT data for the reaction of FeO^+ with CH_4 at 294 ± 3 K in helium buffer gas at a total pressure of 0.47 ± 0.01 mbar in the SIFT apparatus. The solid lines represent a fit of the experimental data to the solution of the set of differential equations for reactions 2a and 2b as well as the subsequent association of CH_4 to $FeOH^+$ to yield $(CH_4)FeOH^+$.

according to Eq. (2) is not observed in this experiment. The corresponding absolute rate constant for the reaction of FeO^+ with CH_4 amounts to $k_{CH_4} = (7.4 \pm 2.2) \times 10^{-11}$ cm^3 s^{-1}, which is again significantly lower than the previously published ICR value, but in good agreement with the revised value obtained after recalibration of the ICR data (see above). Further, under the relatively high pressure of helium, $FeOH^+$ undergoes rapid association with another CH_4 molecule to yield $(CH_4)FeOH^+$, while clustering of Fe^+ with CH_4 is almost negligible under SIFT conditions [43]. Adduct formation of FeO^+ itself seems to be too slow to compete with oxidation of CH_4, although the $(CH_4)FeO^+$ ion has been characterized as a stable species in chemical ionization mass spectrometry [7]. Notably, the branching ratio between reactions 2a and 2b is quite different in the SIFT experiment in that formation of Fe^+ prevails over that of $FeOH^+$ (and $(CH_4)FeOH^+$), i.e., $Fe^+:FeOH^+ = 82:18$. This qualitative difference from the ICR and GIB results turns out to be independent of the CH_4 flow, and within the pressure regime studied (0.40–0.60 mbar), the helium pressure in the flow tube does practically not at all affect the branching ratio (Fig. 6).

4.2. Discussion

Consistent with the findings for reaction 1, the previous ICR measurement [6] leads to a rate constant for reaction 2 which is too high when compared to the SIFT results. Upon re-calibration of the ICR both experiments are brought to agreement with each other; also the GIB value, though somewhat lower, is almost within the error bars of the SIFT data. The comparison of the data for reactions 1 and 2 (Table 3) shows the internal consistencies of the three methods in that the relative reactivities of hydrogen and methane (k_{H_2}/k_{CH_4}) towards FeO^+ are similar in these instruments, though the absolute rate constants differ slightly. However, the finding that the deviation of the GIB to the ICR and SIFT data

is similar for reactions 1 and 2 indicates that underestimation of the rate constants in the GIB apparatus due to a kinetic energy release is in fact negligible, considering that reaction 2 is much less exothermic than reaction 1.

Despite this reasonable agreement in terms of rate constants, the branching ratios for reactions 2a and 2b are similar in ICR and GIB (39:61 and 29:71 respectively), but strikingly different in the SIFT measurements (81:19). Although one may again argue about the possible effects of internal energies in the different machines, we have demonstrated for reaction 1 that these are minor and cannot explain the observed discrepancies. Further, though the energy dependence of the
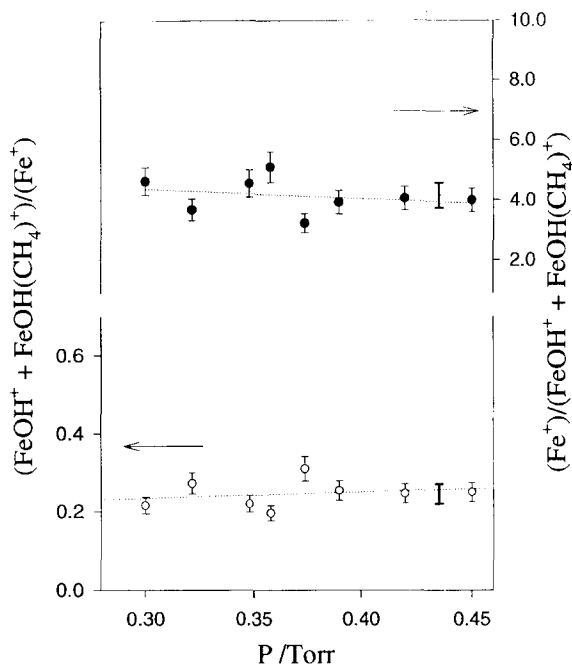

Fig. 6. Measured helium-pressure dependence of the branching ratio for the production of $FeOH^+$ and Fe^+ from the reaction of FeO^+ with CH_4 under SIFT conditions. The dashed lines represent least-square fits to the data. The solid error bars represent standard deviations from the mean and the individual error bars represent an estimation of the absolute error in each single determination. The secondary product-ion signal of $FeOH(CH_4)^+$ has been added to the primary-ion signal of $FeOH^+$ to take into account the further reaction of this ion. The straight lines represent the mean, the solid error bars represent the standard deviation from the mean and the individual error bars represent the absolute error in the determination of the branching ratio.

Table 3
Rate constants (in 10^{-11} cm^3 s^{-1}) for the reactions of FeO$^+$ with hydrogen (k_{H_2}) and methane (k_{CH_4}), branching ratios between Fe$^+$ and FeOH$^+$ in the reaction with methane, and relative reactivities of H$_2$ and CH$_4$ in the ICR, GIB, and SIFT experiments

	k_{H_2}	k_{CH_4}	Fe$^+$:FeOH$^+$	k_{CH_4}/k_{H_2}
ICR	1.0 ± 0.4	8.5 ± 2.6	39:61	8.5
GIB	0.35 ± 0.10^a	2.8 ± 0.8	29:71	8.0
SIFT	0.88 ± 0.26	7.4 ± 2.2	81:19	8.4

[a] The GIB value for the reaction of D$_2$ was converted to that for H$_2$, assuming that the kinetic isotope effect is negligible.

branching ratio is significant, extrapolation of the GIB data (Fig. 4) to even lower energies renders it unreasonable that a slight further decrease of the collision energy should *reverse* the branching ratio in favor of Fe$^+$ formation, as it is observed in the SIFT experiments.

A more probable explanation for the different branching ratios becomes apparent upon inspection of the potential-energy surface for reaction 2 (Fig. 7): after formation of the encounter complex **1**, the rate-determining step of reaction 2 does probably correspond to a C-H bond activation of methane across the Fe$^+$-O bond via the transition structure TS **1/2** to yield the insertion intermediate **2** (together with a spin–flip). This species can then either directly dissociate to FeOH$^+$ + CH$_3^·$ (reaction 2b) or undergoes another rearrangement via TS **2/3** to the product complex **3**, which eventually dissociates to Fe$^+$ and

methanol. Further, formation of Fe$^+$(^{6}D) is slightly exothermic ($\Delta H_R = -9 \pm 2$ kcal mol^{-1}) while that of FeOH$^+$ is almost thermoneutral ($\Delta H_R^0 = -2 \pm 3$ kcal mol^{-1}) [44]. Because the insertion intermediate **2** and the product complex **3** represent stable species in the gas phase [7] and the excess energy is small when these are formed via reaction 2, their lifetimes will be considerable. Therefore, **2** and **3** may experience collisional cooling in the SIFT apparatus before dissociating into the products, even though cooling is not efficient enough to allow for formation of stable **3**. As a consequence, the reactive intermediates are partially quenched in favor of the low-energy channel 2. In contrast, ICR and GIB measurements are performed under strict single-collision conditions, such that stabilization of the intermediates *after* surmounting TS **1/2** is practically impossible. This reasoning accounts well for the fact that the rate constants are similar in all three experimental set-ups, while the branching ratios differ significantly, simply as a result of the higher operating pressures in SIFT mass spectrometry as compared to ICR and GIB. Hence, we expect that at even higher pressures also **2** and/or **3** should be observed as products of reaction 2.

Finally, the discrepancy concerning the observation of reaction 2c should briefly be discussed. Experimentally, FeCH$_2^+$ was only observed under
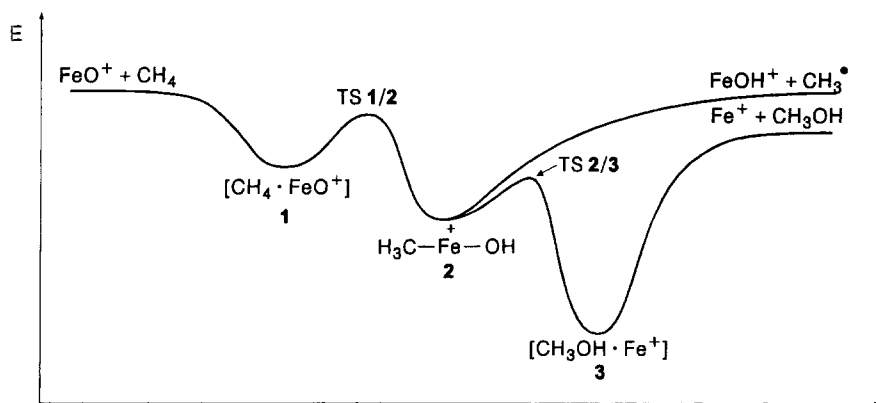

Fig. 7. Qualitative potential-energy surface for the formation of FeOH$^+$ and Fe$^+$ in the reaction of FeO$^+$ with CH$_4$. No details related to the spin multiplicity of the surfaces are included, and there should be two curve crossings as indicated in Fig. 1; for further details, see [3,7,13]b,[14].

ICR conditions, and the accurate mass determination leaves no doubt about its formation from FeO^+. Though one may argue that due to the low mass resolution of the quadrupole analyzers used in GIB and SIFT, the $FeCH_2^+$ product might have been overlooked in the feet of the incident FeO^+ beam, we carefully searched for reaction 2c in these instruments and the upper limit for the branching ratio to yield $FeCH_2^+$ amounts to $< 0.2\%$ in both instruments. In fact, there exist two uncertainties with respect to the origin of this product in the ICR experiments, and these are due to the very low efficiency of reaction 2c: to begin with, at the low operating pressures of the ICR experiments interferences due to background contaminants may become important [45], because several hydrocarbons, e.g., ethene [46], react with FeO^+ to yield $FeCH_2^+$. In fact, at very long reaction times some minor products were observed which indicate the presence of small amounts of background hydrocarbons, e.g., ca. 1% $FeC_3H_6^+$ while trapping FeO^+ for 6 min in 1.8×10^{-8} mbar methane (i.e. $> 99.5\%$ conversion of FeO^+). Moreover, the $FeCH_2^+$ signal is too weak in intensity to allow for a precise analysis of the reaction kinetics of its formation. Due to these uncertainties, the formation of $FeCH_2^+$ as a genuine product of the reaction of FeO^+ with a methane molecule under ICR conditions cannot be warranted, although its formation would be exothermic ($\Delta H^{\circ}_R = -7$ kcal mol^{-1}) and also chemically feasible [6,7].

5. Conclusions

Reliable kinetic data for ion–molecule reactions are of fundamental relevance for the development of gas-phase chemistry in general. In particular, reactions of FeO^+ have implications for systems in the condensed phase, in which iron-oxo moieties are involved as catalytically active species for C–H and C–C bond activation. Here, we have demonstrated that three entirely different experimental techniques reveal the same intrinsic reactivity for FeO^+ towards hydrogen and methane in the gas phase. The previously apparent deviations in the rate constants can be traced back to experimental uncertainties as well as erroneous calibrations, and the rate constants nicely converge to the SIFT results, which provide absolute rate constants. Moreover, the three techniques supplement each other and lead to a uniform description of reactions 1 and 2. Despite this agreement, even more accurate methods to determine rate constants are needed to provide, e.g., more precise intermolecular kinetic isotope effects which would then allow for an analysis of the reaction mechanisms in more detail. As far as ion temperatures are concerned, all methods can provide thermal data, but while thermalization is inherent to the SIFT technique and straightforward for GIB conditions, if a flow tube source is used several precautions have to be taken into account in ICR experiments. Ion thermalization has to be verified carefully for each reactant ion. Moreover, even though thermalization can be achieved by the use of pulsed-valves, no generalization is warranted, because quenching of excited ions may be too ineffective to be performed in ICR.

While the experimentally measured rate constants can be brought into harmony, the branching ratios for reaction 2 cannot. Instead, the analysis of the experiments indicates an influence of the operating pressure on the product distributions *after* the rate-determining transition structure has been achieved, such that the low-energy pathways have a higher propensity in the SIFT experiments. While it is obvious that overall pressure may effect rate constants for termolecular stabilization, it was not envisaged that pressure also may change branching ratios of bimolecular gas-phase reactions which have rate constants independent of pressure. This particular finding has implications for the use of gas-phase data in the kinetic modeling of chemical systems (e.g. interstellar clouds, planetary ionospheres, atmospheres etc.) in which physical conditions can be very different from laboratory

conditions. Thus, critical evaluations of the experimental conditions as well as the potential-energy surface of the reaction of interest are indicated in the comparison of branching ratios obtained under single-collisions and higher pressures.

Finally, we would like to propose reactions 1 and 2 as benchmark reactions for other experimentalists studying ion–molecule reactions, because they possess several desirable features: (i) the generation of FeO^+ (either from $Fe(CO)_5$ or the bare metal) is straightforward and the ion yields are reasonable; (ii) reactions 1 and 2 are easy to perform and to monitor in almost any experimental set-up, and the rate constants are moderate such that they allow for accurate determinations; (iii) unlike many other ions which are frequently used for calibration (e.g. $Ar^{+\cdot}$, $O_2^{+\cdot}$, $CH_4^{+\cdot}$), the FeO^+ ion does *not* react with typical background gases in vacuum systems such as air or water; only residual hydrocarbons (e.g. oil vapor) can deteriorate the results; (iv) the endothermic formation of $FeOH^+$ from FeO^+ and H_2 provides a clear-cut measure for the presence of highly excited ions; (v) ion thermalization can be monitored in reaction 1 via the formation of $FeOH^+$ and the negative temperature/energy dependence of the rate constant without the need for an absolute reference; (vi) the effect of termolecular stabilization can be assessed by the branching ratio of reactions 2a and 2b; (vii) last, but not least, reactions 1 and 2 are interesting in their own right, and further experiments may help to unravel the interplay between "classical" barriers on a single-spin surface and curve-crossing in organometallic chemistry. In this respect, measurements at temperatures much lower than room temperature are particularly desirable.

Acknowledgements

References

[1] M.M. Kappes and R.H. Staley, J. Phys. Chem., 85 (1981) 942.
[2] D. Schröder, A. Fiedler, M.F. Ryan and H. Schwarz, J. Phys. Chem., 98 (1994) 68.
[3] D.E. Clemmer, Y.-M. Chen, F.A. Khan and P.B. Armentrout, J. Phys. Chem., 98 (1994) 6522.
[4] V. Baranov, G. Javahery, A.C. Hopkinson and D.K. Bohme, J. Am. Chem. Soc., 117 (1995) 12801.
[5] T.C. Jackson, D.B. Jacobson and B.S. Freiser, J. Am. Chem. Soc., 106 (1984) 1252.
[6] D. Schröder and H. Schwarz, Angew. Chem., Int. Ed. Engl., 29 (1990) 1431.
[7] D. Schröder, A. Fiedler, J. Hrušák and H. Schwarz, J. Am. Chem. Soc., 114 (1992) 1215.
[8] D. Schröder and H. Schwarz, Angew. Chem., Int. Ed. Engl., 34 (1995) 1973.
[9] K. Weissermel and H.J. Arpe, Industrielle Organische Chemie, VCH, Weinheim, 1988.
[10] P.R. Ortiz de Montellano (Ed.), Cytochrome P-450: Structure, Mechanisms and Biochemistry, Plenum, New York, 1986. D.H.R. Barton, A.E. Martell and D.T. Sawyer (Eds.), The Activation of Dioxygen and Homogeneous Catalytic Oxidation, Plenum, New York, 1993. G.A. Olah and A. Molnár, Hydrocarbon Chemistry, Wiley, New York, 1995.
[11] R.H. Crabtree, Chem. Rev., 95 (1995) 987.
[12] If not mentioned otherwise, thermochemical data were taken from: S.G. Lias, J.E. Bartmess, J.F. Liebman, J.L. Holmes, R.D. Levin and W.G. Mallard, Gas Phase Ion and Neutral Thermochemistry, J. Phys. Chem. Ref. Data, 17 (1988) Suppl. 1. For FeO^+, we used $\Delta H_f = 260$ kcal mol^{-1} according to: S.K. Loh, E.R. Fisher, L. Lian, R.H. Schultz and P.B. Armentrout, J. Phys. Chem., 93 (1989) 3159.
[13] (a) A. Fiedler, J. Hrušák, W. Koch and H. Schwarz, Chem. Phys. Lett., 211 (1993) 242. (b) A. Fiedler, D. Schröder, S. Shaik and H. Schwarz, J. Am. Chem. Soc., 116 (1994) 10734.
[14] S. Shaik, D. Danovich, A. Fiedler, D. Schröder and H. Schwarz, Helv. Chim. Acta, 78 (1995) 1393.
[15] (a) K. Eller and H. Schwarz, Int. J. Mass Spectrom. Ion Processes, 93 (1989) 243. (b) K. Eller, W. Zummack and H. Schwarz, J. Am. Chem. Soc., 112 (1990) 621.
[16] (a) K.M. Ervin and P.B. Armentrout, J. Chem. Phys., 83 (1985)

166. (b) R.H. Schultz and P.B. Armentrout, Int. J. Mass Spectrom. Ion Processes, 107 (1991) 29.

[17] (a) G.I. Mackay, G.D. Vlachos, D.K. Bohme and H. Schiff, Int. J. Mass Spectrom. Ion Phys., 36 (1980) 259. (b) A.B. Raksit and D.K. Bohme, Int. J. Mass Spectrom. Ion Processes, 55 (1983) 69.

[18] Although it was reported in Ref. 5 that FeO^+ does not react with methane, this result turned out to be due to an experimental error, and the occurrence of reaction 2 was later confirmed by Freiser's group, who found a rate constant k_{CH_4} of ca. 1×10^{-10} cm^3 s^{-1} which is in good agreement with the present results; personal communication B.S. Freiser, see footnote 23 in Ref. 6.

[19] R.A. Forbes, F.H. Laukien and J. Wronka, Int. J. Mass Spectrom. Ion Processes, 83 (1988) 23.

[20] M.M. Kappes and R.H. Staley, J. Am. Chem. Soc., 103 (1981) 1286.

[21] J.E. Bartmess and R.M. Georgiadis, Vacuum, 33 (1983) 149.

[22] (a) N.G. Adams, D. Smith and J.F. Paulson, J. Chem. Phys., 72 (1980) 288. (b) B.D. Nourse and H.I. Kenttämaa, J. Phys. Chem., 94 (1990) 5809.

[23] (a) M.T. Bowers, W.J. Chesnavich and W.T. Huntress Jr., Int. J. Mass Spectrom. Ion Phys., 12 (1973) 357. (b) Y. Lin, D.P. Ridge and B. Munson, Org. Mass Spectrom., 26 (1991) 550.

[24] D. Schröder, Dissertation, TU Berlin D83, 1993.

[25] R.H. Schultz, K.C. Crellin and P.B. Armentrout, J. Am. Chem. Soc., 113 (1991) 8590.

[26] Nitrogen oxide thermochemistry is taken from the JANAF tables: M.W. Chase Jr., C.A. Davies, J.R. Downey Jr., D.J. Frurip, R.A. McDonald and A.N. Syverud, J. Phys. Chem. Ref. Data, 14 (1985), Suppl. 1.

[27] P.B. Armentrout, L.F. Halle and J.L. Beauchamp, J. Chem. Phys., 76 (1982) 2449.

[28] Y.-M. Chen and P.B. Armentrout, unpublished results.

[29] (a) R.H. Schultz and P.B. Armentrout, J. Chem. Phys., 96 (1992) 10467. (b) F.A. Khan, D.E. Clemmer, R.H. Schultz and P.B. Armentrout, J. Phys. Chem., 97 (1993) 7978. (c) E.R. Fisher, B.L. Kickel and P.B. Armentrout, J. Chem. Phys., 97 (1992) 4859. (d) E.R. Fisher, B.L. Kickel and P.B. Armentrout, J. Phys. Chem., 97 (1993) 10204. (e) Y.-M. Chen and P.B. Armentrout, Chem. Phys. Lett., 210 (1993) 123. (f) N.F. Dalleska, K. Honma and P.B. Armentrout, J. Am. Chem. Soc., 115 (1993) 12125.

[30] (a) L.J. De Koning, Proefschrift, Universiteit van Amsterdam, 1989. (b) M. Moini and J.R. Eyler, Int. J. Mass Spectrom. Ion Processes, 87 (1989) 29.

[31] T.F. Magnera and P. Kebarle, in M.A. Almoster Ferreia (Ed.), Ionic Processes in the Gas Phase, Reidel, Dordrecht, 1984, p. 135.

[32] The SIFT results were recently confirmed independently, see: J.M.C. Plane and R.J. Rollason, J. Chem. Soc., Faraday Transactions, in press.

[33] For an example, see: F. Strobel and D.P. Ridge, J. Phys. Chem., 93 (1989) 3635.

[34] D. Schröder and H. Schwarz, Angew. Chem., Int. Ed. Engl., 29 (1990) 1433.

[35] Note that due to the low reaction efficiency, also thousands of non-reactive collisions with molecular hydrogen occur until the conversion of FeO^+ is practically complete.

[36] (a) K. Tanaka, J. Durup and I. Koyano, J. Chem. Phys., 74 (1981) 5561. (b) I. Dotan and W. Lindinger, J. Chem. Phys., 76 (1982) 4972. (c) M. Hamdan, K. Birkinshaw and N.D. Twiddy, Int. J. Mass Spectrom. Ion Processes, 62 (1984) 297.

[37] V.G. Anicich, J. Phys. Chem. Ref. Data, 22 (1993) 1469.

[38] For reaction 4 the overestimation of the rate constant may in part be due to different sources for the relative sensitivity \Psi of the ion gauge for N_2O, because this is not included in Ref. 21 and was taken from: F. Nakao, Vacuum, 23 (1975) 431.

[39] The supplier (Balzers, Switzerland) also recommends the values published in Ref. 21.

[40] In the CMS 47X the ion gauge is positioned directly at the front end of the analyzer's turbomolecular pump in a distance of ca. 60 cm from the leak valves, while the ICR cell is ca. 90 cm away in a dead flansch.

[41] C.L. Haynes and P.B. Armentrout, Organometallics, 13 (1994) 3480.

[42] Y.-M. Chen, P.B. Armentrout, J. Chem. Phys., 103 (1995) 618.

[43] H. Becker, Dissertation, TU Berlin D83, 1995.

[44] (a) BDE(Fe^+-OH) was taken as 85 kcal mol^{-1}, see Ref. 3. (b) Also see: T.F. Magnera, D.E. David and J. Michl, J. Am. Chem. Soc., 111 (1989) 4100.

[45] M.F. Ryan, A. Fiedler, D. Schröder and H. Schwarz, Organometallics, 13 (1994) 4072.

[46] D. Stöckigt, Diplomarbeit, TU Berlin, 1991.